Pharm Res (2012) 29:594–602
DOI 10.1007/s11095-011-0590-7

RESEARCH PAPER

Discrimination Between Silicone Oil Droplets and Protein Aggregates in Biopharmaceuticals: A Novel Multiparametric Image Filter for Sub-visible Particles in Microflow Imaging Analysis

René Strehl • Verena Rombach-Riegraf • Manuel Diez • Kamal Egodage • Markus Bluemel • Margit Jeschke • Atanas V. Koulov

Received: 27 June 2011 / Accepted: 13 September 2011 / Published online: 27 September 2011

ABSTRACT

Purpose Accurate monitoring of the sub-visible particle load in protein biopharmaceuticals is increasingly important to drug development. Manufacturers are expected to characterize and control sub-visible protein particles in their products due to their potential immunogenicity. Light obscuration, the most commonly used analytical tool to count microscopic particles, does not allow discrimination between potentially harmful protein aggregates and harmless pharmaceutical components, e.g. silicone oil, commonly present in drug products. Microscopic image analysis in flow-microscopy techniques allows not only counting, but also classification of sub-visible particles based on morphology. We present a novel approach to define software filters for analysis of particle morphology in flow-microscopic images enhancing the capabilities of flow-microscopy.

Methods Image morphology analysis was applied to analyze flow-microscopy data from experimental test sets of protein aggregates and silicone oil suspensions.

Results A combination of four image morphology parameters was found to provide a reliable basis for automatic distinction between silicone oil droplets and protein aggregates in protein biopharmaceuticals resulting in low misclassification errors.

Conclusions A novel, custom-made software filter for discrimination between proteinaceous particles and silicone oil droplets in flow-microscopy imaging analysis was successfully developed.

KEY WORDS biopharmaceuticals · microflow imaging · pre-filled syringes · protein aggregation · silicone oil · subvisible particles

ABBREVIATIONS

AR	aspect ratio
MFI	microflow imaging
NA	numerical aperture
PBS	Phosphate buffer saline
TFA	trifluoroacetic acid

INTRODUCTION

Sub-visible particles, inherently present in all protein drugs, have recently become the focus of attention for the health authorities (1) owing to the widely spread notion that microscopic protein aggregates may be harmful when injected into humans due to their potential immunogenicity (2,3). In consequence, sub-visible particles are considered an important safety-related quality attribute of biopharmaceuticals and manufacturers are expected to monitor the formation of sub-visible particles in their products during manufacturing and long-term storage. Until recently,

Electronic supplementary material The online version of this article (doi:10.1007/s11095-011-0590-7) contains supplementary material, which is available to authorized users.

R. Strehl · V. Rombach-Riegraf · M. Diez · K. Egodage · M. Bluemel · M. Jeschke · A. V. Koulov
Analytical R&D, Biologics Process R&D, Technical R&D
Novartis Pharma AG
Basel, Switzerland

A. V. Koulov (✉)
Novartis Pharma AG, Werk Klybeck
WKL-693.2.139.17
CH-4002, Basel, Switzerland
e-mail: atanas.koulov@novartis.com

analytical techniques based on light obscuration were the only widely applied technology to measure sub-visible particles in pharmaceutical products. This methodology is based on the ability of a particle to reduce the measured light intensity when passing a light beam. Whereas standard light obscuration instruments are able to count particles larger than 1–2 μm, a major disadvantage of this technique remains the lack of ability to discriminate between the different classes of particles present in a test solution.

This functionality is needed especially for particle monitoring and characterization in drug products filled in syringes. Pre-filled syringes are the preferred primary packaging format for liquid therapeutic proteins due to the convenience of administration. However, syringes usually have a thin layer of silicone oil applied to the inner surface of their barrel as lubricant in order to ensure smooth gliding of the plunger. A certain amount of silicone oil always partitions into the aqueous drug solution forming small, sub-visible oil droplets. Although silicone oil is inert and considered harmless to humans, these microscopic silicone oil droplets are indistinguishable from the potentially harmful proteinaceous particles by conventional light obscuration measurements. This puts forward the need to develop techniques that allow the differentiation of silicone oil droplets from proteinaceous particles.

Flow microscopy techniques are gaining an increasing popularity for particle analysis owing to their ability to capture digital images of the particles present in solution. Computer analysis of these particle images does not only allow accurate counting, but also classification of the particles based on their morphology (4,5). Currently, there are several flow microscopy instruments available on the market representing different technical implementations of essentially the same principle. For this study, Microflow Imaging or MFI (Brightwell Technologies, Ottawa, Canada) was used as it offers a good compromise between counting accuracy and image quality. Briefly, in MFI bright-field images are captured in successive frames by a high-speed camera as a continuous sample stream passes through a flow cell positioned in the field of view of a microscopic system. This setup allows counting of all particles present in the solution in the size-range from 2 μm to 400 μm. The digital images of all particles may be examined to further classify the particles based on their morphology and level or translucency. Silicone oil droplets for example, have a very characteristic appearance in the MFI images due to their perfectly spherical shape and the particular way they refract light (6,7). Interestingly, while there are routines available for the MFI instrument software to process the image morphology data, a fast and reliable software filter for automatic classification of oil *versus* non-oil particles is still lacking. Here we present a novel approach to the development of such software filter, based on a combination of four image parameters that serves as a reliable basis for discrimination between silicone oil droplets and proteinaceous particles. The utility of such procedures was confirmed using test sets of protein and silicone oil particles larger than 2 μm.

MATERIALS AND METHODS

Materials

The MFI DPA4100 series A (Brightwell Technologies, Inc., Canada) equipped with a 470 nm LED light source was used to detect and measure particles. Phosphate buffer saline (Dulbecco's, pH 6.5) was purchased from Invitrogen™, 0.22 μm disposable MILLEX®GP filter units from Millipore (Carrigtwohill, Ireland) and NIST traceable standards were obtained from Duke Scientific (Fremont, CA). HELLMANEX®II protein cleaning solution was purchased from Hellma® Analytics (Germany), filtered pipette tips from Mettler-Toledo International Inc., small volume tubes from Nalgene® Cryoware™, large volume tubes (Cellstar® Tubes) from Greiner bio-one, silicone oil from Hach-Lange (Germany) and trifluoroacetic acid from PIERCE. A thermo mixer "Comfort" from Eppendorf was used in the heating studies and a "Clima Temperatur System" from CTS (Germany) for the freeze/thaw trials. Two antibodies (Novartis development products)—IgG-A (showing relatively low aggregation propensity) and IgG-B (showing relatively high aggregation propensity) were used as model proteins.

Preparation of Aggregates

Using pH Stress

5 mL aliquot of 150 mg/mL protein solution was transferred into a tube with a volume at least twice of the sample volume for proper mixing. While vortexing the solution 25 μl of trifluoroacetic acid (TFA) were added to reach a final TFA concentration of 0.5% (*v*/*v*). After vortexing the sample for further 30 s, the TFA spiked sample was shaken for 30 min in a horizontal position at room temperature and 300 rpm. 1 mL of this sample was measured.

Using Heat/Shaking Stress

1 mL of filtered, undiluted antibody solution (150 mg/mL) was transferred into a tube. The samples were stressed for 10 min at 60°C and 1,400 rpm and stored on dry ice until the measurement.

Using Freeze/Thaw Stress

4.5 mL of unstressed and diluted protein solution (2 mg/mL in PBS) were filtered through a 0.22 µm filter and transferred into a 5 mL tube. Using a software program the sample was frozen and thawed automatically. Ten freeze/thaw cycles were performed. The samples were equilibrated to 4°C for 20 min before and after each cycle. One cycle was defined as following: temperature decrease from 4°C to −40°C within 30 min, holding time at −40°C for 25 min, temperature increase from −40°C to 30°C within 35 min, followed by a holding time of 25 min at 30°C and finally, a temperature decrease from 30°C to 5°C within 5 min.

Preparation of Silicone Oil Spiked Samples

To prepare a "silicone oil only" sample, a 5 mL aliquot of unstressed and undiluted antibody solution (150 mg/mL) was filtered through a 0.22 µm filter. 20 mg silicone oil were added using a pipette. To ensure good homogenization, this sample was shaken for 3 h in a horizontal position at room temperature and 300 rpm. To prepare stressed protein sample spiked with silicon oil 4 mL of aggregated material (see above) was spiked with 20 mg of silicone oil. To ensure good homogenization, the spiked sample was agitated as described above.

Microflow Imaging Measurements

The system was flushed with 15 mL of HELLMANEX II (2%) solution and with 15 mL of water. For these flushing steps a silanized glass syringe (15 mL) was used. The flow rate was set to maximum speed. This flushing step was repeated after each different sample.

1 mL of all samples was filtered and degassed (>30 min, 20 mbar) prior to each measurement and were used to perform the "optimization of illumination" routine. Using a portion of the sample, which is filtered directly prior use, in order to perform "optimization of illumination" is essential for high image quality and results in low misclassification errors of the filter.

The samples were gently mixed and degassed (>30 min, 20 mbar). 1 mL of each sample was measured. A maximum number of images was collected during each measurement.

Calculation of S-Factors and Assessment of Errors in Particle Identification

The S-factor for each individual particle was determined by calculating the multiplication product of the values of these four optical parameters for oil and protein particles separately: Circularity, Aspect Ratio, Object Intensity STD, Object Intensity MAX. These S-factors were sorted by size (ECD) and their average values, as well as their standard deviation in each individual size bin were calculated. The averages were used to determine and calculate the S-factor Cut-Off function:

$$Cut\ off_{specific\ size} = Avg.[Oil_{specific\ size}] - \frac{Avg.[Oil_{specific\ size}] - Avg.[Protein_{specific\ size}]}{2}$$

Based on these cut-off values, the errors (per size bin) were calculated by counting all oil particles below the cut-off and all protein particles above the cut-off. The total numbers of incorrectly classified particles (for both protein and oil) were then related to the total number of detected oil particles:

$$error_{oil,specific\ size} = 100 - \left[\frac{\#\ of\ counts\ within\ avg._{S-factors,\ specific\ size,\ oil} \pm STD_{oil}}{Total\ \#\ of\ counts_{oil}}\right]$$

The calculation of the protein specific errors is equivalent:

$$error_{protein,\ size\ bin} = 100 - \left[\frac{\#\ of\ counts\ within\ avg._{S-factors,\ specific\ size,\ protein} \pm STD_{protein}}{Total\ \#\ of\ counts_{protein}}\right]$$

The cut-off values were then optimized manually for each size range in order to obtain errors below 5%. Further, using non-linear regression function fitting the final cut-off parameters were defined as follows: 2.13 µm–4.38 µm (S-factor = 36375*ln(x)-23108 (R^2=1)); 4.63 µm–10.88 µm (S-factor = 38767*ln(x)-27428 (R^2=1)); 11.13 µm–400 µm (S-factor = 72000 (R^2=1)).

After the calculation of the S-factor for each individual particle, classification in two categories (*"oil"* and *"non-oil"*) was performed by sorting these particles according to the calculated cut-off values (S-factor higher than the cut-off—"oil," S-factor lower than the cut-off—"non-oil").

Finally, the percentages of oil and protein were calculated by counting all particles classified as "oil" or "protein," respectively (per specific size bin).

Defintions of MFI image parameters are presented in Table I.

RESULTS AND DISCUSSION

In order to assess the prospect of developing a software filter for discrimination between silicone oil droplets and proteinaceous particles, samples containing only silicone oil droplets (suspended in filtered protein solution) and

Table I Definitions of MFI Image Parameters

Parameter	Definition
Aspect ratio	A value between zero and one (unit-less) that represents the ratio of theminor axis length over the major axis length of an ellipse that has the same second- moments as the particle.
Circularity	A value between zero and one (unit-less) that represents the ratio of the circumference of an equivalent area circle over the measured perimeter.
Equivalent circular diameter (ECD)	It is expressed in microns and represents the diameter of a sphere that occupies the same two-dimensional surface area as the particle.
Intensity MAX	The maximum illumination intensity (brightest pixels) of a particle expressed in 1,023 levels of intensity.
Intensity STD	The standard deviation of the illumination intensity levels in a particle. In the case of MFI, a 10 bit sensor is used which provides 1,023 levels of intensity resolution.

artificially stressed protein samples containing only protein particles, respectively, were prepared (see Materials and Methods). These samples were analyzed by MFI. Upon close examination of the MFI images it becomes evident that silicone oil droplets and proteinaceous particles appear sufficiently different to the human eye even at sizes close to the lower size limit of the instrument (sizes as low as 2.13 μm) (see Fig. 1). This observation leads to the conclusion that a reliable discrimination of particles larger than 2 μm in two categories (oil and protein) based on their image parameters should be possible.

Indeed, in a recent publication such an approach using the image parameter aspect ratio (AR) was proposed and reported to result in misclassification of about 5% for particles larger than 5 μm (7). In our hands, when applying this filter to a number of proteins and stress conditions the reported performance of the filter could not be confirmed. In some cases, the misclassification errors were larger than 40%. In addition, these errors increased significantly at lower sizes as protein particles, similarly to silicone oil droplets, have aspect ratio close to 1.0, as previously pointed out by Oma and colleagues (7). As a consequence of the latter observation, the proposed AR filter would only be partially applicable to protein biopharmaceuticals, where the vast majority of the particles are smaller than 5 μm due to the exponential decay distribution of particle

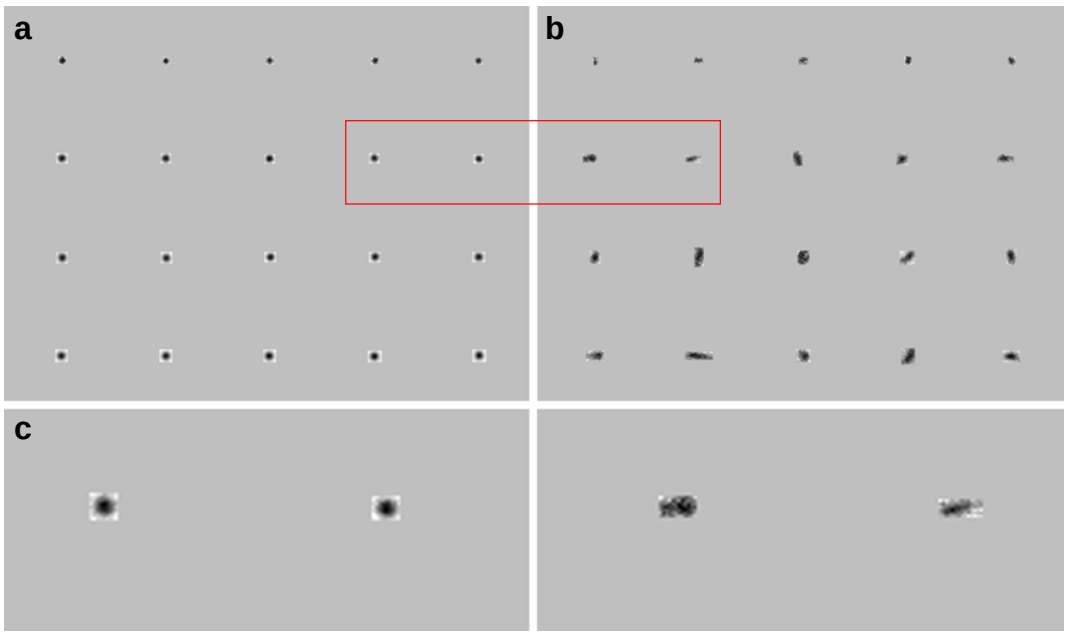

Fig. 1 A collage of representative silicone oil droplets (**a**) and IgG-A protein particles (**b**) of sizes: 2.13 μm (first row from top **a** and **b**), 3.13 μm (second row from top **a** and **b**), 4.13 μm (third row from top **a** and **b**), and 5.13 μm (fourth row from top **a** and **b**). Ten randomly selected particles of each size class are shown. Solution of IgG-A was filtered through a 0.22 μm filter which was followed by addition of silicone oil (see Materials and Methods) (**a**). Protein particles were generated by shaking a solution of IgG-A at 60°C for 10 min at 1,400 rpm in the absence of silicone oil (**b**). The area delimited in *red* is shown in **c** zoomed; silicone oil droplets (*left*) and protein particles (*right*) show the differences in morphology of both classes of particles even in this small size—3.13 μm.

numbers with size (the smaller the size—the larger the number of particles present in solution) (8,9).

Upon a systematic review of all nine individual image parameters and the distribution of their values in samples containing either oil droplets only or protein particles only (see Materials and Methods) one finds a very significant overlap between these values for protein aggregates and silicone oil droplets in the size range between 2 µm and 15 µm.

The most discriminating image parameter is *aspect ratio* (see Fig. 2). However, the distributions of the values observed for protein aggregates and for silicone oil droplets reveal a high risk of wrong classification.

Despite the well-separated average values, the large spread of the individual values (reflected by the error bars) prohibits an accurate differentiation between these two particle classes, especially for sizes smaller than 5 µm, where the errors (misclassification) range up to 50% (see Fig. 3). Furthermore, the morphology of proteinaceous particles strongly varies depending on the stress condition used to generate them (see Fig. 4). Most importantly, the particles formed using stress conditions relevant to the real storage conditions for biopharmaceuticals (heat, shaking, freeze/thawing) have the highest aspect ratio and are therefore the most difficult to distinguish from silicone oil droplets when only this parameter is used.

An alternative approach to address this problem would be to apply multivariate statistical analyses in order to assess how a given image parameter varies with relation to other image parameters and size. In this article, we present a third, multiparametric approach using a custom function derived from several MFI image parameters that we selected (aspect ratio, circularity, maximum object intensity and standard deviation of object intensity—for exact definitions see Materials and Methods).

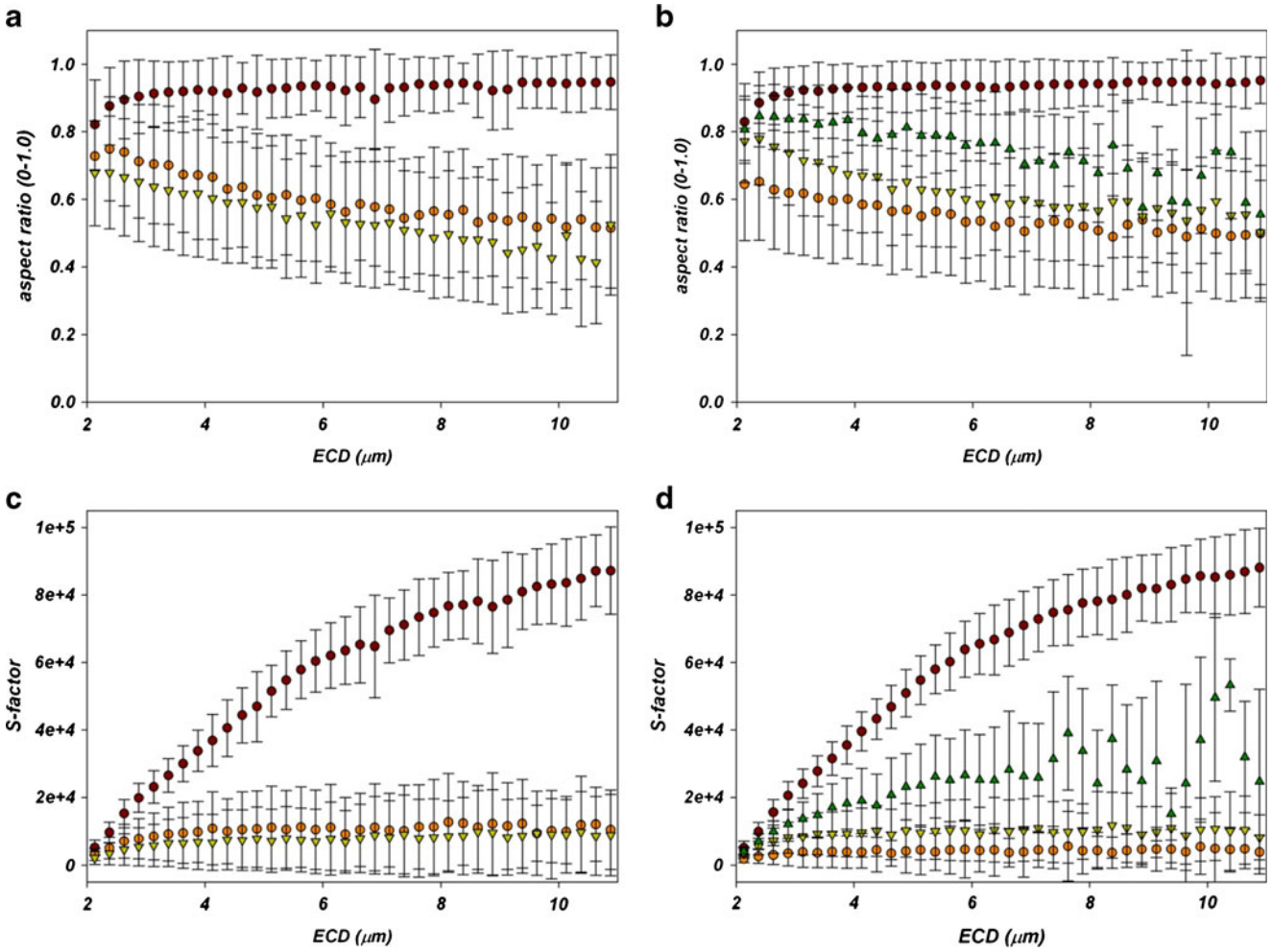

Fig. 2 Graphical representation of the size distribution of the image parameter *aspect ratio* (**a**—IgG-A and **b**—IgG-B) and S-factor (**c**—IgG A and **d**—IgG-B) for protein particles and oil droplets obtained using MFI (see Materials and Methods)—average values per size bin with 0.25 µm step ranging from 2.13 µm to 11.13 µm, including the standard deviations (*error bars*). *Brown circles*—oil droplets, *orange circles*—pH stressed protein, *light green triangles*—heat/shaking stressed protein, *dark green triangles*—freeze-thaw stressed protein.

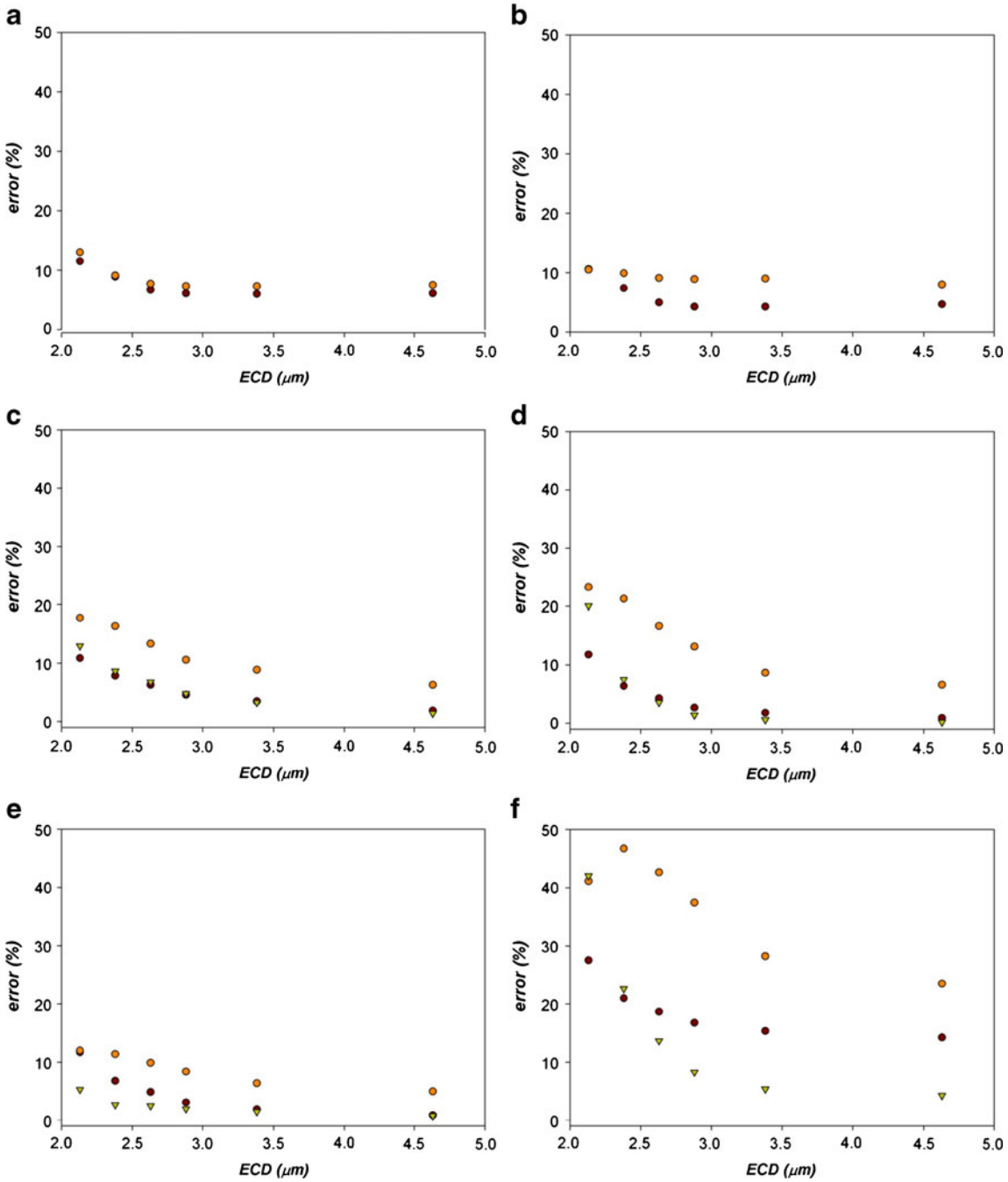

Fig. 3 Misclassification errors of the image analysis filters measured using experimental test sets: (**a**) silicone oil droplets in filtered IgG-A solution, classified as "non-oil" by the filter; (**b**) silicone oil droplets in filtered IgG-B solution, classified as "non-oil" by the filter; (**c**) IgG-A particles produced by heat/shaking stress, classified as "oil" by the filer; (**d**) IgG-B particles produced by heat/shaking stress; (**e**) IgG-A particles produced by pH stress, classified as "oil"; (**f**) IgG-B particles produced by freeze-thawing stress, classified as "oil". For experimental details, see Materials and Methods. In all plots the results from the application of aspect ratio >0.85 filter are shown in *orange circles*, basic S-filter—in *brown circles* and protein specific filter—in *light green triangles*. Tabulated data may be found in Table S1 from Supplementary Material.

Firstly, several parameters which differ significantly for protein aggregates and silicone oil droplets across the size range from 2 μm to 400 μm were identified. As noted above, none of these parameters could provide adequate discrimination between oil and protein on their own. More specifically, while the average values for protein and oil particles were significantly different, the individual values for large number of the particles varied extensively, thus resulting in a considerable overlap. We rationalized that a function, which is a product of the values of several parameters (each showing relatively small value differences between oil and protein particles), must result in sufficiently

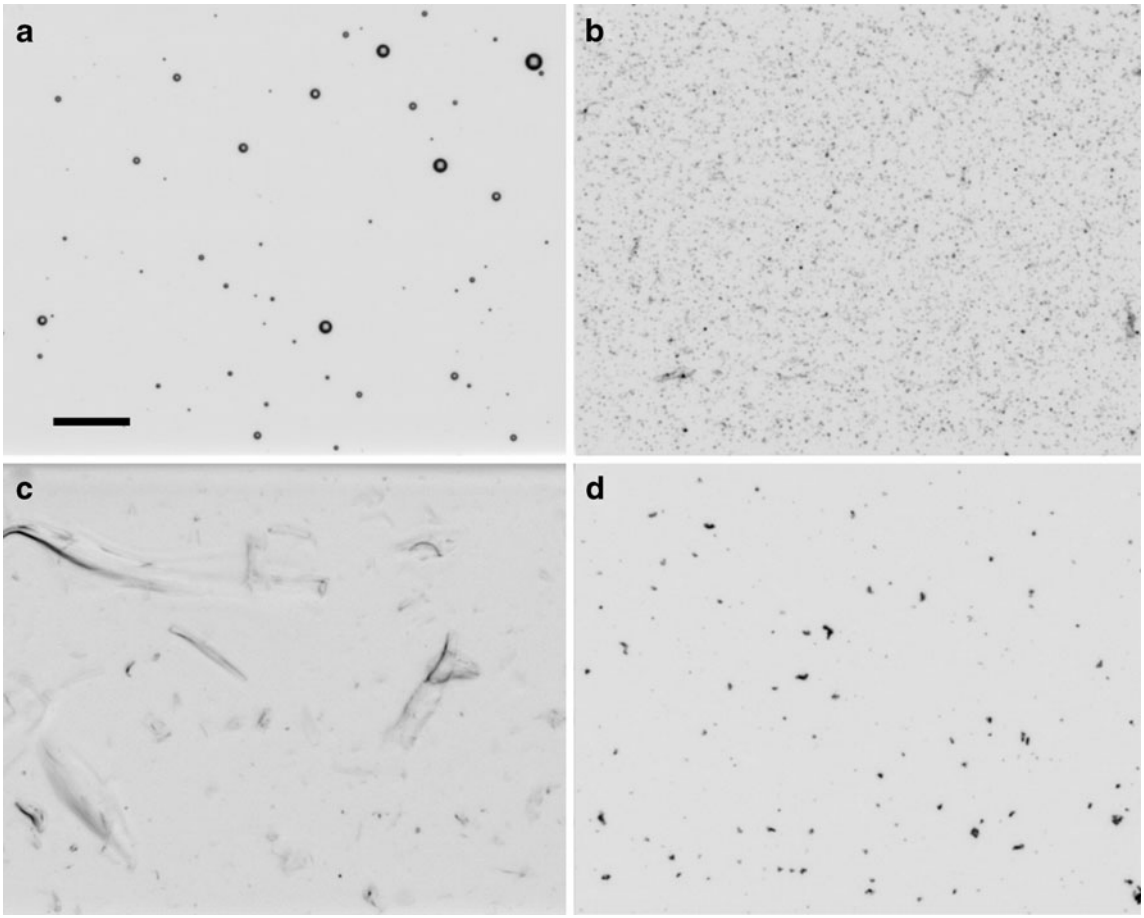

Fig. 4 Representative screenshots of MFI analysis of (**a**) silicone oil in filtered IgG-B solution, (**b**) particles of IgG-B subjected to heat/shaking stress, (**c**) particles of IgG-B subjected to pH stress, (**d**) particles of IgG-B subjected to freeze/thawing stress (for experimental details, please, see Materials and Methods). *Scale bar* corresponds to 200 μm.

large spread and thus provide a more reliable basis for distinction, i.e. while the differences (signal) would be multiplied; the variability (noise) would not.

The parameters selected were aspect ratio, circularity, maximum object intensity and standard deviation of object intensity. This choice was based on the appearance of the silicone oil and proteinaceous particles. As seen in Fig. 4 silicone oil particles are perfectly round (due to their hydrophobicity) and therefore have very high values for circularity and aspect ratio. On the other hand, protein particles even at the lower size ranges are irregular and therefore the values for these parameters for protein would always be lower. In addition, while silicone oil particles appear very dark in the smallest sizes, a characteristic bright spot appears in the middle as they become larger resulting in an increasingly higher maximum object intensity. Larger silicone oil droplets always maintain this characteristic appearance in water, buffers and even in the presence of proteins (for examples see Supplementary Material). The presence of very dark and very bright pixels in the images of silicone oil droplets contributes to their significantly larger values of standard deviation of the object intensity. Based on these observations one expects that multiplying the image parameters together with their differences in values would allow better separation of the populations of oil droplets and protein particles. Consequently, they might be used as a software filter to discriminate between these two populations in samples containing both types of particles. According to this assessment, a custom function (*S-factor*) was defined as the product of multiplication of the values of the parameters aspect ratio, circularity, maximum object intensity and standard deviation of object intensity (see Materials and Methods).

In order to assess the performance of the software filters described here, experimental test sets were created using either stressed protein solutions not containing any silicone oil ("protein only") or stressed protein solutions which were filtered using 0.22 µm filter in order to remove all sub-visible particles and to which subsequently silicone oil was added ("silicone oil only"). These samples were analyzed using MFI DPA4100 (see Materials and Methods) and the images were subsequently evaluated. The S-factor filter and the aspect

ratio (AR) filter were applied on the same datasets to classify all particles in the samples as either "non-oil particles" or "oil droplets." The errors given by the software filters were defined as follows: Err_{prot} was defined as the fraction of all particles in the protein only sample classified by the software filter as "silicone oil droplets" and Err_{oil}—the fraction of the particles in the oil only sample classified as "non-silicone oil particles."

The distribution of the S-factor for the two different proteins used in this study as well as the variation of the aspect ratio for the same (both per MFI size bin) are depicted in Fig. 2 using the average values per MFI size bin as well as their relative standard deviations. Upon comparison of the two variables it becomes evident that much larger spread between the values of the S-factors of the smallest sizes (<10 μm) is observed as compared to the one between the values of aspect ratio. This spread allows for defining a cut-off function (see Fig. 2) in order to classify each particle as either "non-oil" or "oil" according to the value of its S-factor. Further, comparison between the errors of the two filters (see Fig. 3) reveals that the S-factor filter in all cases results in smaller Err_{prot}—in most cases at least twice as small and in some cases 33 times smaller than the previously proposed AR filter. Interestingly, these differences vary, depending on: a) individual proteins and b) type of stress applied to generate aggregates. These observations are rationalized after examination of the images of protein particles generated by different types of stress. For example, particles generated by pH stress are much more dissimilar from silicone oil droplets as compared to particles made by heat/shaking or freeze-thawing (see Figs. 2 and 4).

After analyzing a number of data sets obtained for different proteins from the Novartis pipeline as well as different stress conditions, a cut-off function was defined for a basic silicone oil filter (see Materials and Methods). However, as the particle morphology varies slightly from protein to protein (for particles formed under identical stress conditions), the filters may be further optimized for individual proteins by tuning the cut-off function to further reduce the misclassification errors (see the examples in Fig. 3).

Using the approach outlined above it is possible to create a large number of custom image analysis filters based on different combinations of nine image parameters that MFI offers. For example, if three out of nine image parameters are used there are 84 possible combinations; if four out of nine image parameters are used there are 126 combinations possible, and so on to give a total of 511 combinations. In order to validate the software filter proposed here, all possible combinations of the nine image parameters were assessed. Firstly, S-factors were calculated for both protein particles and silicone oil droplets for all size-bins from 2.13 μm to 400 μm in 0.25 μm steps for a test set. Secondly, a cut-off function was defined in each case, taking the median of the difference between the average S-factors for protein particles and silicon oil droplets in each size-bin. Finally, the errors (overlap) in these S-factors for both particle types (protein particles classified as oil or oil droplets classified as protein particles) in the corresponding size bin were determined.

Using this systematic approach all theoretically possible software filters based on combinations of particle image parameters were compared. This assessment established that indeed the combination proposed initially (*i.e.* aspect ratio, circularity, maximum object intensity and standard deviation of object intensity) provides the best possible discrimination (lowest misclassification errors) for protein and silicone oil particles.

Yet surprisingly, several other parameter combinations were found to result in very good discrimination between protein particles and silicone oil droplets. This finding is particularly encouraging in terms of future development of software filters for flow microscopy, as the values of the different image parameters may vary significantly from protein to protein (depending on the shape of the particles formed under stress). Although the latter is contrary to our own experience, having multiple options for filter development in the future (utilizing different combinations of image parameters) gives researchers the opportunity to apply this approach to their specific products and problems. Regardless of variations in the image filters that we may see in the future, the fundamental principle of using several parameters in order to multiply the "signal" and cancel out the "noise" that we propose here is likely to remain widely applicable in particle image analysis the future. Furthermore, the filter proposed here provides the opportunity to compare datasets generated in different laboratories and standardize this type of analysis.

Light obscuration has a lower size limit of detection of approximately 1–2 μm, which is imposed by the limit of sensitivity of the photodiode of the detector. In contrast, flow microscopy is capable of counting and imaging even smaller particles. For an optical system with a numerical aperture of the objective close to 1.0, high magnification and a high resolution camera the theoretical optical resolution would be approximately the wavelength, which in MFI is 470 nm, divided by 2. However, the depth of field of such a system would be far too small to be of practical use when trying to image particles in a flow cell on the order of hundreds of microns in depth. Operating at a lower numerical aperture and magnification offers a trade-off between the lower size limit and the practical measurement range of the system. For the DPA 4100 MFI system used in this work, this results in an operating range to measure particles between 2 and 400 μm. We expect that in the future, if such highly sensitive hardware setup

becomes available, it may be possible to discriminate between silicone oil droplets and proteinaceous particles smaller than 1 μm by using the image morphology analysis approach that we offer here.

It probably is worth mentioning, that the distribution of the intensity image parameters (e.g. Object Intensity MAX, Object Intensity STD) may differ in future hardware versions of MFI in case a different wavelength of illumination is implemented. Since both light absorption and refractive indices are wavelength-dependent, the level of opaqueness of the particles may vary slightly (for examples see Supplementary Material), which in such modified instrument versions would need to be assessed.

Finally, the approach applied here was an empirical one. While it has resulted in the development of filters with excellent accuracy, it is likely that in the future multivariate statistical analysis would find wider use. The implementation of such statistical tools in the software package of instruments would be very beneficial to the broad application of flow microscopy to the sub-visible particle analysis in the biopharmaceutical industry.

CONCLUSION

In conclusion, we have demonstrated the successful development and use of a novel, custom made software filter for discrimination between proteinaceous particles and silicone oil droplets in flow-microscopy imaging analysis. The new filter is based on a multiparametric approach and uses four MFI image morphology parameters simultaneously. This novel methodology was evaluated using in parallel experimental test sets of different proteins, generated using several different types of physical stress, as well as silicone oil suspensions. The results presented here demonstrate that the novel software filter allows reliable classification of silicone oil and proteinaceous particles as small as 2 μm with relatively low errors.

ACKNOWLEDGMENTS & DISCLOSURES

We would like to thank Christian Reithmaier for his support with MS Excel.

REFERENCES

1. Rosenberg AS. Effects of protein aggregates: an immunologic perspective. AAPS J. 2006;8(3):E501–7.
2. Carpenter JF, Randolph TW, Jiskoot W, Crommelin DJ, Middaugh CR, Winter G, *et al.* Overlooking subvisible particles in therapeutic protein products: gaps that may compromise product quality. J Pharm Sci. 2009;98(4):1201–5.
3. Singh SK, Afonina N, Awwad M, Bechtold-Peters K, Blue JT, Chou D, *et al.* An industry perspective on the monitoring of subvisible particles as a quality attribute for protein therapeutics. J Pharm Sci. 2010;99(8):3302–21.
4. Wuchner K, Büchler J, Spycher R, Dalmonte P, Volkin DB. Development of a microflow digital imaging assay to characterize protein particulates during storage of a high concentration IgG1 monoclonal antibody formulation. J Pharm Sci. 2010;99(8):3343–61.
5. Liu L, Ammar DA, Ross LA, Mandava N, Kahook MY, Carpenter JF. Silicone oil microdroplets and protein aggregates in repackaged bevacizumab and ranibizumab: effects of long-term storage and product mishandling. Invest Ophthalmol Vis Sci. 2011;52(2):1023–34.
6. Sharma DK, King D, Oma P, Merchant C. Micro-flow imaging: flow microscopy applied to sub-visible particulate analysis in protein formulations. AAPS J. 2010;12(3):455–64.
7. Sharma D, Oma P, Krishnan S. Silicone micro-droplets in protein formulations—detection and enumeration. Pharm Technol. 2009;33(4):74–9.
8. Mahler HC, Friess W, Grauschopf U, Kiese S. Protein aggregation: pathways, induction factors and analysis. J Pharm Sci. 2009;98(9):2909–34.
9. Huang CT, Sharma D, Oma P, Krishnamurthy R. Quantitation of protein particles in parenteral solutions using micro-flow imaging. J Pharm Sci. 2009;98(9):3058–71.